Size and shape of three-dimensional Cu clusters on a MgO(001) substrate: Combined *ab initio* and thermodynamic approach

David Fuks,[1] Eugene A. Kotomin,[2,3] Yuri F. Zhukovskii,[2] and A. Marshall Stoneham[4]

[1]*Materials Engineering Department, Ben-Gurion University of the Negev, P. O. Box 653, Beer-Sheva, Israel*

[2]*Institute for Solid State Physics, University of Latvia, Kengaraga 8, LV-1063 Riga, Latvia*

[3]*Max-Planck-Institut FKF, Heisenbergstr. 1, D-70569 Stuttgart, Germany*

[4]*Center for Materials Science, Department of Physics and Astronomy, University College London, Gower Street, London WC1E 6BT, United Kingdom*

In order to describe theoretically metallic island growth at the early stages of metal deposition on oxide substrates, we combined *ab initio* atomic and electronic structure calculations with thermodynamic theory of solid solutions. The experimentally observed truncated pyramidal shape of metallic clusters is reproduced as the result of metal atom segregation from the lattice gas in imaginary Ising lattice towards the metal/substrate interface. Our approach is illustrated by detailed analysis of Cu islands on a MgO(001)-terminated surface. We predict dependencies of the shape and the height of such clusters on the temperature and metal gas pressure.

Nanometer-size metal particle growth on metallic or oxide substrates is relevant for micro- and nanoelectronics, optical devices, and catalysis.[1,2] Control of metal particle size and shape plays here a vital role. It is well recognized nowadays that during epitaxial growth of Ag, Cu, and Pd thin films on MgO substrate, three-dimensional (3D) metallic clusters begin to grow already at submonolayer coverages.[2,3] Grazing incidence small-angle x-ray scattering experiments[2–5] indicate that these clusters have a shape of a *truncated pyramid or octahedron*. A pyramidal island shape is expected on all substrates with fourfold atomic coordination, for example, (001) surfaces of fcc oxides (e.g., Refs. 4–6). A schematic view of such cluster is shown in Fig. 1(a).

In the past, *kinetics* approaches (Ref. 7 and references therein) have given very successful understanding of metal on ionic (oxide) morphologies. Recently, we developed the complementary *thermodynamic* approach[8–10] based on the *ab initio* energetics of the metal/oxides interfaces. We studied there the initial stages of the Cu or Ag cluster growth on MgO(001) substrate at submonolayer coverages by combining atomic/electronic structure calculations with the theory of spinodal decomposition in a two-dimensional (2D) solid solution of "adatom-empty lattice site (E) (Cu/Ag-E)" (the adsorbate first plane embedded into the electrostatic field of the substrate). We have shown that at moderate temperatures and corresponding compositions in a Cu/Ag-E solid solution on the phase diagram, the system turns out in the region between solvus and spinodal, which leads to a two-phase mixture of extremely compact 2D metallic islands and practically empty-site regions. For example, at $T \approx 550$ K the isolated 2D Cu islands with the local atomic fraction 0.997 of Cu are formed, whereas the mean concentration of Cu on the MgO substrate was varied from 0.02 to 0.15 [see Fig. 6(b) in Ref. 8]. In this paper exploring the idea of the lattice gas on the Ising lattice,[9,10] we extend our approach on *ab initio* thermodynamics of 3D Cu cluster formation on a MgO(001) surface. Our study is based on a synthesis of (i) the results of our *ab initio* calculations,[8] (ii) the ideas of Bozzolo-Ferante-Smith (BFS) for the atomistic modeling of

surface alloys,[11] and (iii) thermodynamic theory of the segregation in binary solid solutions. The uniqueness of our thermodynamic approach is its ability to predict the *size and shape* of the growing 3D clusters at different concentrations of the metal atoms in the vapor above the MgO substrate and at different temperatures.

In order to study growth of 3D metallic islands, we consider an imaginary lattice above (i.e., away from the semi-bulk) the MgO surface. In this imaginary lattice, Cu atoms can diffuse, rather like a gas of Cu atoms on a discrete lattice (in other words, this is "Cu atom-empty lattice site" solid solution). These atoms experience interactions with the MgO substrate and with each other. The formation of 2D metallic clusters of Cu (Ref. 8) on MgO may be considered as the
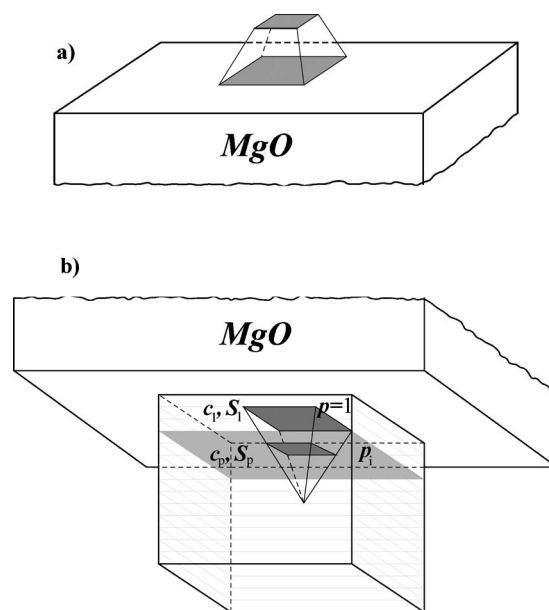

FIG. 1. (a) Schematic view of the 3D Cu cluster on MgO(001) substrate, and b) imaginary lattice with dense Cu layers forming the pyramidal 3D metallic cluster during the segregation onto the substrate.

segregations of Cu onto the first plane of such Ising lattice. These 2D clusters serve in fact as the nuclei of 3D Cu islands. The identity of the thermodynamic approaches for the segregation and adsorption at the interface is discussed in Ref. 12. It is well known that when the surface segregation of a component A (Cu, in our case) on the surface of A–E (E stands for empty sites) alloy occurs, *the concentration profile* of surface segregation for this component decreases from the surface inwards the bulk.[13]

Following Ref. 11, we introduce the *active computational cell*, namely, a small sample of the real Cu/MgO interface. In this cell we choose the region on the MgO substrate that is pure Cu (this is justified by our above-mentioned studies[8–10]). We aim to investigate *equilibrium* states rather than kinetics, so we do not look at the rate at which a Cu on the surface might climb on top of a cluster of N layers. In the same spirit, we allow layer by layer to grow, subject to rules and energies, first of all, the conservation of the total Cu concentration in the N-layer computation cell. The calculation scheme[14–16] was used here. As follows from our *ab initio* study,[8] Cu atoms prefer to occupy positions above O atoms. For this reason the lattice parameter of the Ising lattice above the MgO(001) substrate was chosen equal to the O-O distance on the MgO(001) surface.

Each imaginary lattice layer $p=1,2\dots$ in the cell is characterized by the average metal concentration c_p, and the area, S_p, it covers [Fig. 1(b)]. Since we assume dense 3D metallic clusters, the following relation takes place:

$$S_{p+p'}/S_p = c_{p+p'}/c_p, \quad p,p' = 1,2,3\dots. \quad (1)$$

In the basal plane of such 3D Cu island concentration $c_1=1$, whereas at its top $c_{p\gg1}=c_{vap}$, where c_{vap} corresponds to the atomic fraction of Cu in the vapor reservoir representing the computational cell. Thus, the height of the islands is defined by the shape of the *concentration profile* for the surface segregations in Cu-E 3D solid solution. Let us discuss now how to obtain the size and shape of 3D cluster at different temperatures based on a thermodynamic approach.

Several alternative approaches exist in the configurational thermodynamics methods for describing the surface concentration profiles for segregation in surface solid solutions and alloys. The advantages and disadvantages of these approaches as combined with first-principles calculations of interaction in the alloys are discussed in Ref. 13.

Here we choose the *free-energy concentration expansion method* (FCEM).[14,15] This statistical-mechanical analytical approach, based on the Ising model Hamiltonian, is known to agree with Monte Carlo (MC) results much better than the standard Bragg-Williams theory. It is quite accurate and simple to apply, demanding much less computational effort compared to MC or cluster variation methods. In FCEM, additional terms of the higher orders in the site occupation numbers are included into the free energy, in order to account for the correlation effects in alloys.

Using the Ising model in which "spin" variables $\{\sigma_i\}$ describe the site occupations, we set σ_i equal to 1 (−1) provided the site i is occupied by a Cu atom, or it is empty. The Cu-E alloy configurational energy can be written as in Refs. 15 and 17:

$$E = \frac{1}{2}\sum_p \left(\sum_{m \in p\text{-}layer} \Delta H_p^s \sigma_m \right) + \frac{1}{2}\sum_{\{mn\}} V_{mn}(\sigma_m \sigma_n - 1). \quad (2)$$

By analogy with the phenomenological models,[18–20] ΔH_p^s accounts for atomic size mismatch (e.g., elastic) energy. We treat the atomic size mismatch energy in the first layer ΔH_1^s in the same way as in Ref. 8 whereas ΔH_p^s for $p \geq 2$ following Ref. 17. To the first approximation and similarly to a study[17] on Pt_cNi_{1-c} alloys, the difference in tensions between constituents within the p layer, Δh_p is neglected. V_{mn} in Eq. (2) is the effective pair interaction (*mixing potential*) defined in terms of the interaction energies between the corresponding quasiparticles, V_{mn}^{CuCu}, V_{mn}^{EE}, and V_{mn}^{CuE}, at the sites m and n in the Cu-E solid solution. Symbol $\{mn\}$ denotes a pair of lattice sites, whereas

$$V_{mn} = \frac{1}{2}(V_{mn}^{CuCu} + V_{mn}^{EE} - 2V_{mn}^{CuE}). \quad (3)$$

Keeping in mind that $\langle\sigma_m\rangle = 2C_m - 1$, where C_m is the occupation probability of the lattice site m,[21] and that the Bragg-Williams (BW) *configurational entropy* for a random alloy may be presented as a sum over layers (with N_p sites in pth layer),

$$S^{BW} = -k\sum_p N_p[c_p \ln(c_p) + (1-c_p)\ln(1-c_p)], \quad (4)$$

after averaging Eq. (2) over all possible configurations, the configurational free energy in the BW-type approximation may be written down as

$$F^{BW'} = kT\sum_p N_p[c_p \ln(c_p) + (1-c_p)\ln(1-c_p)]$$

$$+ \frac{1}{2}\sum_p [N_p(\Delta h_p + \Delta H_p^s)(2c_p - 1)]$$

$$+ \frac{1}{2}\sum_{\{mn\}} V_{mn}[(2C_m - 1)(2C_n - 1) - 1]. \quad (5)$$

In our case, N_p is the same for all layers of the simulation cell [see Fig. 1(b)]. c_p is C_m averaged over all lattice sites in the layer p. In our case of absolutely disordered Cu-E solid solution in the computation cell, all C_m values are equivalent within the same layer, and c_p are just equal to C_m if the site m belongs to the layer p. However, this is not true in the general case, e.g., when the sites in a layer are inequivalent due to existence of several sublattices.

The correlation effects leading to the short-range pattern formation are considered in the FCEM through the expansion of the short-range order contribution into the free energy, ΔF^{SRO}, in the reverse-temperature power series on cumulants.[22] This term in the nearest neighbor approximation reads:[14]

$$\Delta F^{SRO} = -kT \sum_{\{mn\}} C_m(1-C_m)C_n(1-C_n) \left[\exp\left(-\frac{2V_{mn}}{kT}\right) \right. $$
$$\left. + \frac{2V_{mn}}{kT} - 1 \right]. \tag{6}$$

For more mathematical details, we refer the readers to Ref. 23, where the correlation effects in ordering alloys were discussed, and to Ref. 24 where analogous results for "atom-vacancy" solid solutions were considered.

The total configurational free energy of the Cu-E random solid solution is

$$F = F^{BW'} + \Delta F^{SRO}. \tag{7}$$

Lastly, the probability of finding the nearest Cu-Cu pair on the Ising lattice sites m and n is given by[14]

$$p_{mn} = C_m C_n - C_m(1-C_m)C_n(1-C_n) \left[1 - \exp\left(-\frac{2V_{mn}}{kT}\right) \right], \tag{8}$$

which obviously differs from a simple product $C_m C_n$, for the pair probability in a completely random solid solution. The occupation probability of the n site by the Cu atom provided the site m is also occupied by Cu, is $\tilde{p}_{mn} = p_{mn}/C_m$. In Eqs. (2)–(8) the indices $\{mn\}$ run not only over the sites within the same layer p, but also between nearest layers: $(p, p+1)$ for $p=1$ and $(p, p-1, p+1)$ for $p>1$.

In order to obtain the mixing potential V_{mn}, we have performed *ab initio* calculations[8] using the CRYSTAL-2003 code.[25] In these calculations we have used the DFT-HF hybrid Becke 3-Parameter, Lee, Yang and Parr (B3LYP) exchange-correlation functional and localized atomiclike Gaussian functions. We have optimized the Cu basis set using small core Hay-Wadt pseudopotentials, whereas Mg and O have been treated as all-electron ions (see more details in Ref. 8). Briefly, the procedure of extracting the mixing potential is based on the calculations of the internal formation energies for several completely ordered superstructures that may be formed in two-dimensional (2D) Cu-E solid solution above the (001)-terminated MgO substrate.[8–10] The chosen structures are stable with respect to formation of antiphase domains according to the Lifshitz criteria.[26] The internal formation energies for these superstructures may be expressed in terms of Fourier transforms, $\tilde{V}(\vec{k})$, of the mixing potential $V_{mn}^{CuCu} + V_{mn}^{EE} - 2V_{mn}^{CuE}$. Our calculations demonstrated that these structures are energetically unfavorable with respect to the ground state which is a mixture of the components of 2D solid solution weighted with their atomic fractions. Solving the set of equations for the internal formation energies for these structures, the Fourier transform $\tilde{V}(0)$ corresponding to $\vec{k}=0$ was obtained. As shown in Refs. 9 and 10, $\tilde{V}(0)$ is a key energy parameter defining the solubility or decomposition of disordered solid solution at finite temperatures.

The $\tilde{V}(0)$ calculated in this way accounts for the charge redistribution in 2D solid solution immersed in the field of the (001)-terminated MgO substrate.[9,10] In Ref. 8 we went beyond the standard solid solution approximation, and found

that this potential depends on the *atomic fraction* of Cu in a 2D solid solution. The existence of the concentration-dependent term in the potential appears as the result of the *ab initio* optimization of the distance between the Cu monolayer and the MgO substrate. The $\tilde{V}(0)$ could be well fitted to the function

$$\tilde{V}(0) = -0.6858 - 0.0823c \, (\text{eV}), \tag{9}$$

being negative for all Cu concentrations (c stands here for the concentration of Cu in the 2D solid solution). This allowed us to calculate the "temperature-composition" phase diagram of 2D Cu-E solid solution. We demonstrated in Ref. 8 the decomposition of such solid solutions at finite temperatures and predicted the formation of 2D dense Cu islands in the region between the binodal and spinodal.

To generalize here our approach,[8–10] let us consider now the growth of 3D Cu clusters above the 2D Cu islands in terms of the segregation of Cu in the vicinity of the (001)-terminated MgO substrate, and use Eqs. (5), (6), and (7). Using the $\tilde{V}(0)$ obtained from *ab initio* calculations, we define the effective mixing potential, V_{mn} [Eq. (3)], for the layer $p=1$ in the *nearest-neighbor approximation*. (Such approximation was used also in Ref. 17 and is justified by the electronic structure calculations for *fcc* alloys.[27]) This gives

$$V_{mn} = \frac{1}{8}\tilde{V}(0) \equiv V_0 = -0.0857 - 0.0103c \, (\text{eV}), \tag{10}$$

where m, n sites lie in the first layer nearest to the surface, $p=1$. Keeping in mind that the effective pair interaction is enhanced at the oxide surface, we use the relation[17]

$$V_{mn} = V_0/1.5, \tag{11}$$

if atoms in n or m, or both sites of the computation cell lie in the deeper metal layers, $p \geq 2$, i.e., in the bulk of 3D Cu-E solid solution. This permits us to transfer the results of the 2D *ab initio* calculations of the effective mixing potential, V_{mn} for the 3D case. Such the generalization is also justified by (a) a very low charge transfer across the Cu/MgO interface which is in fact physisorption,[8] (b) a rather weak dependence of the mixing potential on the atomic fraction of Cu as obtained in our *ab initio* calculations, and (c) the results of the study[15] of the effect of *composition-dependent* interatomic interactions on the surface alloying and on the segregation, where the significant changes in the concentration profiles for Cr segregation on the Fe(100) substrate are found only when V_{mn} *changes sign* (mixing tendency changes to decomposition).

In our calculations we used the computational cell containing $N=10^3$ (001) layers, with 600 sites per layer (that is, about 50 Å × 50 Å), that simulates a thick Cu-E solid solution on the fcc Ising lattice above the substrate. The Cu concentrations in 21 layers above the MgO were varied, in order to find the minimum of the free energy for N-layer surface alloy and to obtain the in-depth layer-by-layer concentration profiles of segregated Cu atoms at different temperatures. In this minimization the total atomic fraction of Cu atoms in the vapor reservoir, c_{vap} was fixed constant ($c_{vap}=0.01$ and $c_{vap}=0.3$).

Following Ref. 15, our model takes into account the dependence of interatomic interactions V_{pq} on the local average concentrations $\tilde{c}_{p,q}$ of metal atoms surrounding the m, n pairs of the lattice sites which could lie either in the same layer or the two nearest layers p and q. In the free energy minimization, along with the direct variation of concentrations within different layers, an indirect variation of the interlayer and in-layer concentration-dependent interactions $V_{pq} = V(\tilde{c}_{p,q})$ [Eqs. (10) and (11)] is also performed. According to Ref. 15, in fcc structure the nearest neighbor (NN) approximation is quite sufficient. The local effective interactions V_{pq} between lattice sites in the (001)-oriented p and q layers ($q = p, p \pm 1$) were calculated here using the average concentrations in the NN environment of each pair of lattice sites. Explicitly, the method[15] was applied, and the equations for the average concentrations were derived. For $p, q = 1$ and $p = 1$, $q = 2$ these average concentrations read

$$\tilde{c}_{1,1} = \frac{1}{14}(8c_1 + 6c_2), \tag{12}$$

$$\tilde{c}_{1,2} = \frac{1}{16}(6c_1 + 6c_2 + 4c_3), \tag{13}$$

whereas for $p > 1$ one easily gets

$$\tilde{c}_{p,p} = \frac{1}{20}(6c_{p-1} + 8c_p + 6c_{p+1}), \tag{14}$$

$$\tilde{c}_{p,p+1} = \frac{1}{20}(4c_{p-1} + 6c_p + 6c_{p+1} + 4c_{p+2}). \tag{15}$$

Let us discuss now results for Cu growth on the MgO substrate. In Fig. 2 the calculated concentration profiles for Cu in a computational cell [Fig. 1(b)] with two vapor concentrations $c_{vap} = 0.01$ and 0.3 are presented at different temperatures. From Fig. 2(a) the conclusion can be drawn that for small Cu concentration in the vapor, the Cu concentrations in a cluster are close to unity at low temperatures only and in several layers very close to the Cu/MgO interface. In the more distant layers the Cu concentration sharply decreases and becomes extremely low, close to $c_{vap} = 0.01$. Substitution of the data on c_p into Eq. (1) gives the relative areas S_p in 3D clusters. For layers remote from the surface $c_p \sim c_{vap}$ and thus a dense Cu layer cannot be formed. This leads to the truncated shape of the metallic cluster as shown schematically in Fig. 1. For relatively small number of atoms in a 3D cluster, its shape preserves the structure of the crystalline lattice and thus should be a pyramidal, rather than conic shape. As the temperature increases, the Cu concentration rapidly decreases in several layers close to interface. The areas of the dense layers decrease as well as the number of the dense layers in the truncated pyramids (Fig. 3). For higher Cu concentrations in a vapor [Fig. 2(b)], the situation is similar, but quantitatively differs in the number of dense areas in the pyramids. Comparing the results for c_p at the same temperature (say, 700 K), we find that the number of the dense layers increases from six to ten, as the vapor concentration increases from $c_{vap} = 0.01$ up to 0.3.
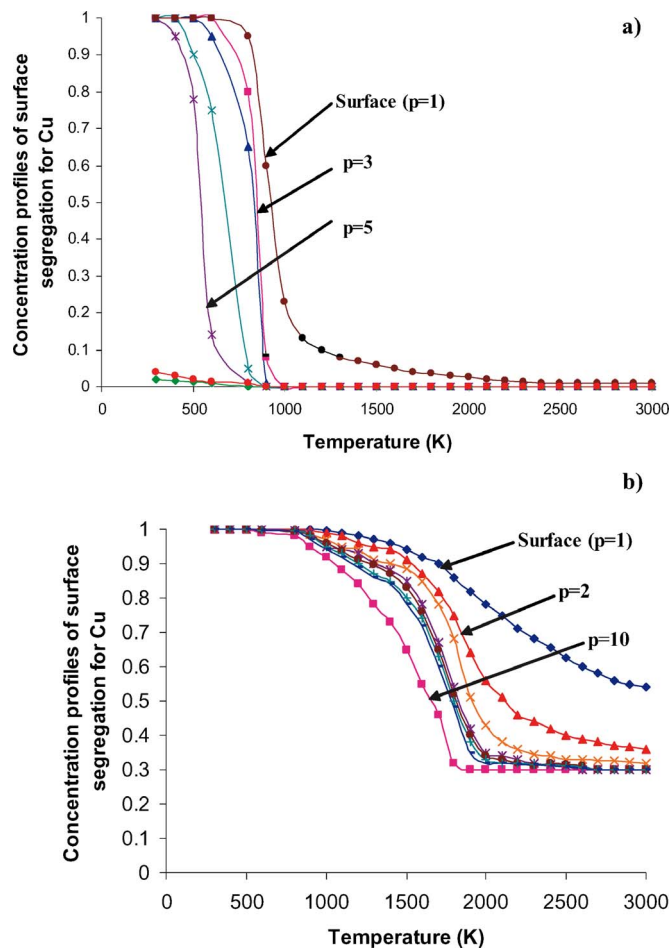

FIG. 2. (Color online) Concentration profiles of Cu segregation on the (001) surface from the semi-infinite Cu-empty site imaginary lattice above the (001) terminated MgO substrate: a) the Cu concentration in a vapor above the substrate (a simulation cell), $c_{vap} = 0.01$, b) the same for $c_{vap} = 0.3$.

In Fig. 4 we present schematically the *shape* of the pyramids obtained at three different temperatures for $c_{vap} = 0.01$. The basal area of the pyramid at $T = 400$ K is taken as unity.
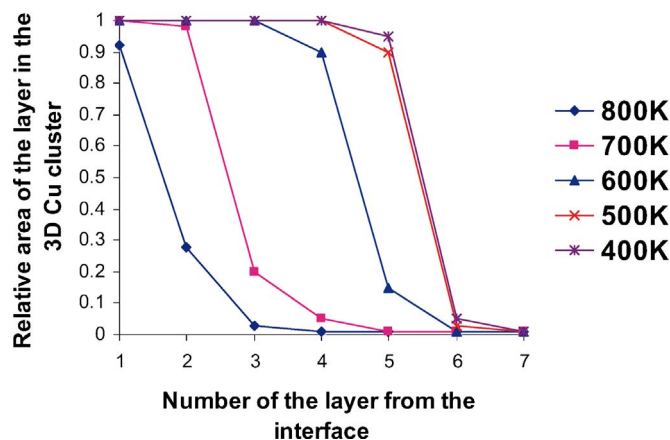

FIG. 3. (Color online) Relative areas of the layers inside 3D Cu clusters on the (001) MgO substrate at the early stage of a Cu deposition. Lines are given to guide the eye.
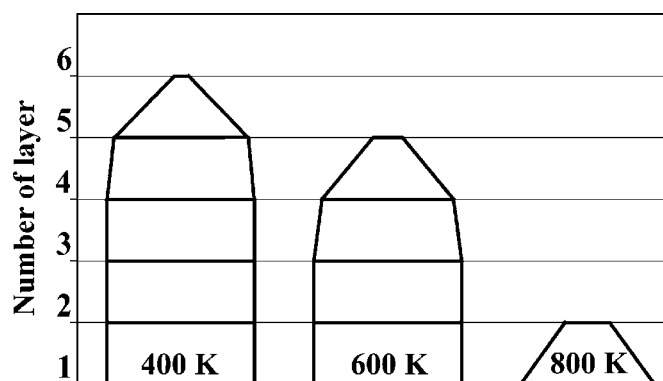
FIG. 4. Schematic shape of 3D Cu cluster for c_{vap}=0.01 at three different temperatures.

At this temperature a Cu cluster has a columnlike shape with a small-height truncated pyramid atop it. As the temperature increases to 600 K, the column height decreases whereas the height of the truncated pyramid increases. The total height of the Cu cluster becomes smaller as well as the number of atoms inside the cluster. Lastly, at T=800 K we observe the truncated pyramid containing only two planes.

The temperature dependence of the height of the cluster is illustrated in Fig. 5, it decreases parabolically from ~10 Å down to ~2 Å. Simultaneously, the area of the basal plane decreases. This means that with the temperature increase the relative amount of atoms in the cluster decreases due to strongly reduced segregation trend. Our results are in good agreement with the interpretation of the experimental data suggested in Ref. 2. Indeed, along with the similar pyramidal shape of the 3D metallic clusters, we have demonstrated that even for relatively low Cu concentration in the vapor, the clusters may grow up several-plane high, which is experimentally observed.[2] The results of our calculations are also in good agreement with the model used for fitting the crystal truncation rods of Ag on MgO(001) (See Fig. 8 in Ref. 4). Experimental check of the predicted temperature dependence could be of great interest.
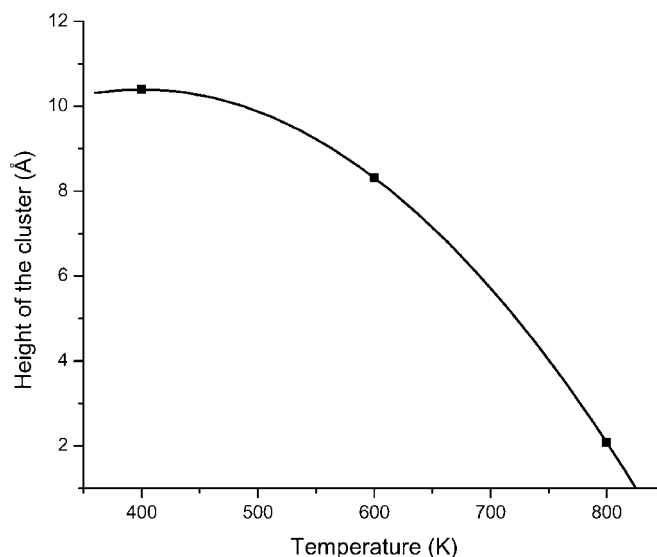

FIG. 5. The temperature dependence of the height of Cu clusters extracted from Fig. 4.

In conclusion, our general approach, based on the combination of the *ab initio* electronic structure calculations and the *thermodynamics of alloy segregation*, permits much more detailed and realistic prediction of the growth of nanosize clusters on ceramic substrates than was possible before. In particular, we go beyond the standard nonempirical approach based on the analysis of the surface energy of the metal[28] linked to the wetting angle by the Young-Dupré relation.[29] The additional advantage of our thermodynamic approach is that it takes into account the metal-substrate interaction.[8]

ACKNOWLEDGMENTS

[1] C. T. Campbell, S. C. Parker, and D. E. Starr, Science **298**, 811 (2002).

[2] G. Renauld, R. Lazzari, Ch. Revenant, *et al.*, Science **300**, 1416 (2003).

[3] J. H. Larsen, J. T. Ranney, D. E. Starr, J. E. Musgrove, and C. T. Campbell, Phys. Rev. B **63**, 195410 (2001).

[4] O. Robach, G. Renaud, and A. Barbier, Phys. Rev. B **60**, 5858 (1999).

[5] A. Barbier, G. Renaud, and J. Jupille, Surf. Sci. **454-456**, 979 (2000).

[6] P. Lagarde, S. Colonna, A.-M. Flank, and J. Jupille, Surf. Sci. **524**, 102 (2003).

[7] H. Brune, Surf. Sci. Rep. **31**, 121 (1998); J. Venables, *Introduction to Surface and Thin Film Processes* (Cambridge University Press, Cambridge, England, 2000).

[8] Yu. F. Zhukovskii, E. A. Kotomin, D. Fuks, S. Dorfman, A. M. Stoneham, and G. Borstel, J. Phys.: Condens. Matter **16**, 4881 (2004).

[9] D. Fuks, S. Dorfman, Yu. F. Zhukovskii, E. A. Kotomin, and A. M. Stoneham, Surf. Sci. **499**, 24 (2002).

[10] D. Fuks, S. Dorfman, E. A. Kotomin, Yu. F. Zhukovskii, and A. M. Stoneham, Phys. Rev. Lett. **85**, 4333 (2000).

[11] G. Bozzolo and J. E. Garces, in *Surface Alloys and Alloy Surfaces*, edited by D. P. Woodruff (Elsevier Science B.V., New York, 2002), pp. 30–85, and references therein.

[12] A. Umantsev, Phys. Rev. B **64**, 075419 (2001).

[13] A. V. Ruban and H. L. Scriver, Comput. Mater. Sci. **15**, 119 (1999).

[14] J. M. Roussel, A. Saul, L. Rubinovich, and M. Polak, J. Phys.: Condens. Matter **11**, 9901 (1999).

[15] M. Polak, C. S. Fadley, and L. Rubinovich, Phys. Rev. B **65**, 205404 (2002).

[16] M. Polak and L. Rubinovich, Surf. Sci. Rep. **38**, 127 (2000).

[17] B. Legrand, G. Tréglia, and F. Ducastelle, Phys. Rev. B **41**, 4422 (1990).

[18] A. R. Miedema, Z. Metallkd. **69**, 455 (1978).

[19] J. R. Chelikowsky, Surf. Sci. Lett. **139**, L197 (1984).

[20] F. L. Williams and D. Nason, Surf. Sci. **45**, 377 (1974).

[21] A. G. Khachaturyan, *Theory of Structural Transformations in Solids* (Wiley, New York, 1983).

[22] J. G. Kirkwood, J. Chem. Phys. **6**, 70 (1938).

[23] D. A. Badalyan and A. G. Khachaturyan, Sov. Phys. Solid State **12**, 346 (1970).

[24] D. Fuks, Comput. Modell. New Technol. **7**, 28 (2003).

[25] V. R. Saunders, R. Dovesi, C. Roetti, R. Orlando, C. M. Zicovich-Wilson, N. M. Harrison, K. Doll, B. Civalleri, I. J. Bush, Ph. D'Arco, and M. Llunell, CRYSTAL 2003 user manual (University of Turin, Italy, 2003).

[26] E. M. Lifshitz, J. Phys. (USSR) **7**, 61 (1942); **7**, 251 (1942).

[27] A. Bieber, F. Gautier, G. Tréglia, and F. Ducastellle, Solid State Commun. **39**, 149 (1981).

[28] M. Alfredsson and C. R. A. Catlow, Surf. Sci. **561**, 43 (2004).

[29] J. M. Howe, Int. Mater. Rev. **38**, 233 (1993).